Delay-induced transitions in visually guided movements

P. Tass,[1] J. Kurths,[2] M.G. Rosenblum,[2,*] G. Guasti,[2] and H. Hefter[1]
[1]*Department of Neurology, Heinrich-Heine-University, Moorenstrasse 5, D-40225 Düsseldorf, Germany*
[2]*Max-Plank-Arbeitsgruppe ''Nichtlineare Dynamik'' an der Universität Potsdam,*
Am Neuen Palais 19, PF-601553, D-14415, Potsdam, Germany
(Received 23 April 1996; revised manuscript received 1 July 1996)

We investigated phase dynamics of sinusoidal forearm tracking with delayed visual feedback. To this end we introduced two data analysis tools which enabled us to find several delay-induced transitions between qualitatively different regimes. Our results show that the investigation of delay-induced transitions of the phase dynamics in tracking movements provides us with insights into the underlying neuronal signal processing. In particular, we experimentally verified predictions of a recently presented mathematical model [P. Tass, A. Wunderlin, and M. Schanz, J. Biol. Phys. **21**, 83 (1995)]. [S1063-651X(96)51009-3]

PACS number(s): 87.22.Jb, 05.45+b

The control of visually guided movements is based on the interactions of visual and proprioceptive feedback. The latter is a consequence of the mechanism of proprioception which continuously provides the brain with information about the muscles' activity and the resulting biomechanical changes.

Feedback can be analyzed in tracking experiments, where a motion has to be synchronized with a visually presented target. In various tracking experiments an artificial delay was introduced in the visual feedback loop in order to analyze visually guided movements (cf. [2]). Tracking with a delay was also used to analyze the oculomotor system alone [3] or the interaction between skeletomotor and oculomotor control [4]. The root mean square error between target and tracking signals [2] and return maps of the pointwise relative phase (to be defined below) [5] were used to quantify the dynamics. In an experiment of Beuter *et al.*, subjects had to maintain a constant finger displacement although a variable time delay was inserted into the visual feedback [6]. With increasing time delays irregular rhythms appeared with short intermittent periods of regular oscillations.

In this paper we present an approach which enables us to reveal qualitatively different dynamical regimes and to analyze the impact of artificial delays on visually guided movements. In particular we show that investigating delay induced transitions of the phase dynamics in tracking movements makes it possible to analyze the underlying neuronal signal processing.

Analyzing the phase of motion turned out to be fruitful several times (for a review, see [7]). In particular we refer to the model of phase transitions in human hand movements presented by Haken *et al*. [8], where the frequency of an oscillatory movement served as control parameter. In our experiments, the artificial delay, which is inserted into the visual feedback loop, serves as control parameter. Variation of this delay gives rise to several bifurcations which are related to characteristic dynamical states.

The complex neuronal interactions which realize the processing of proprioceptive and visual information remain unclear so far. On the other hand, in nonlinear systems with multiple negative feedback loops, extremely complex dynamics may evolve [9]. Thus, in order to be guided to delay-induced movement patterns, a model was developed which is based on a few neurophysiological assumptions [1]. In this paper we introduce two data analysis tools in order to confirm at least qualitatively several of the model's predictions. The comparison between the experimental data and the model's behavior allows us to decide whether the model's assumptions make sense or whether they have to be modified or even rejected.

Next we briefly sketch the experimental setup. For further details we refer to [2,5]. Recordings of sinusoidal forearm tracking with delayed visual feedback were performed with 26 right handed normal subjects (7 female; 19 male; age range: 19–53 yrs; mean age: 28.4 yrs). In the experiment subjects are comfortably sitting in a chair in front of an oscilloscope. With their right arm they grasp a manipulandum handle of low inertia and low friction. Two signals are displayed on the oscilloscope: 1. The *target signal* is a vertical double bar moving sinusoidally in the horizontal direction with a constant frequency. 2. Subjects control the position of a further vertical bar, the so-called *tracking signal*, by means of the manipulandum. To this end the angle of the manipulandum handle is fed into a delay unit and presented with an experimentally controlled delay as horizontal position of the tracking signal on the oscilloscope. Thus, when the manipulandum is shifted to the right for vanishing delay the tracking signal turns to the right and vice versa. Subjects are required to keep the tracking signal in the middle between the moving double bar, so that tracking signal and target signal are synchronized. Target signal, tracking signal, and manipulandum angle are digitized each with 250 Hz and stored for off-line analysis.

The target frequency is the subject's preferred tracking frequency. It is determined in a short preexperimental trial where the oscilloscope is turned off and the subject is asked to perform sinusoidal forearm movements with a most convenient frequency. The preferred target frequency in our group ranges from 0.5 to 0.9 Hz. The target frequency is kept constant throughout the entire experimental session.

*Permanent address: Mechanical Engineering Research Inst., Russian Academy of Sciences, Moscow, Russia.

During a single recording the *relative delay* τ_{rel} is constant. The latter is defined by $\tau_{rel}=\tau/T$, where τ denotes the experimentally controlled delay which is inserted into the visual feedback loop, whereas T is the target period. From trial to trial only the relative delay is pseudorandomly varied. Depending on the subject 9 to 15 different delays are tested over a period of 15 min for each delay. Between the single trials pauses had to be inserted so that the subjects did not become exhausted. The recording session lasted between 2.5 and 4 h.

Along the lines of a *top-down approach*, a model was presented [1] which describes the synchronization process between two oscillators, namely, the oscillating target signal and the oscillatory forearm movement. The derivation of the model equation relies on the following *assumptions*: 1. The amplitude dynamics of the forearm oscillator is neglected in a first approximation. 2. Except for the experimentally controlled delay all other delays are neglected because under physiological conditions they are assumed to be compensated. 3. The control of the tracking movement is based on nonlinear interactions of target signal, tracking signal, and proprioceptive feedback signal. 4. For vanishing delay τ the subject is assumed to track without any mistake. 5. We take into account that healthy subjects are able to reproduce the target frequency. For this reason the eigenfrequency of the forearm oscillator equals the target frequency which is denoted by ω.

Let us denote the target signal, i.e., the target's horizontal position on the oscilloscope, by $s_1(t)=A_1\sin\theta(t)$, where A_1 is constant. Thus, $\dot{\theta}=d\theta/dt=\omega$. Analogously the tracking signal, i.e., the time delayed displayed manipulandum angle, is denoted by $s_2(t)=A_2\sin[\psi(t-\tau)]$, where A_2 in the model is assumed to be constant (cf. assumption 1). τ denotes the artificial delay which is inserted into the visual feedback loop. In order to describe the phase dynamics of the tracking behaviour appropriately, we introduce the *phase difference* ϕ between target signal and tracking signal by putting $\phi(t)=\theta(t)-\psi(t-\tau)$. With these notations we obtain the *model equation*

$$\dot{\phi}(t)=-\underbrace{\alpha\sin[\phi(t)-\omega\tau]}_{\mathrm{I}}-\underbrace{\beta\sin[\phi(t-\tau)]}_{\mathrm{II}}, \tag{1}$$

where α and β are positive real constants [1]. The right-hand side of Eq. (1) reflects two matching processes: Term I corresponds to the matching between target signal and actual forearm position given by the proprioceptive feedback. Term II corresponds to purely visual matching: The subject has to minimize the angular displacement between target signal and tracking signal.

A qualitative analysis of this model leads to the following main *predictions*: 1. *Subcritical shift of the fixed point.* Starting with vanishing delay (i.e., $\tau=0$) and increasing τ causes a shift of the stable fixed point of the phase difference ϕ_0 according to

$$\phi_0=\frac{\omega\tau}{2}+\arctan\left(\frac{\alpha-\beta}{\alpha+\beta}\tan\frac{\omega\tau}{2}\right). \tag{2}$$

2. *Oscillations.* When τ exceeds a critical time delay τ_{crit} a Hopf bifurcation occurs, giving rise to an oscillation of the phase difference ϕ. 3. *Running solutions.* By further increase of the delay running solutions, i.e., infinite growth of phase difference, occur. We denote rather monotonically increasing or decreasing running solutions as ''drifts.'' On the other hand a rather monotonic increase or decrease of ϕ may alternate with small amplitude oscillations confined to one cycle. This type of running solution may be called ''cycle slipping.'' The oscillatory as well as the rather monotonic part of the dynamics may dominate, giving rise to different types of cycle slipping. Delay-induced transitions between the different types of running solutions take place as well. 4. *Chaotic region.* For larger delays the system also exhibits chaotic oscillations with amplitudes confined to one or at most two phase cycles. The determination of the Lyapunov dimension of the delay dependent sequence of attractors showed that limit cycle oscillations or fixed point behavior can be encountered at larger delays (cf. Fig. 11 in [1]).

Now we present two data analysis techniques to investigate the phase dynamics of the experimental data and to check the predictions of the model. The first method aims at continuous determination of the phase difference of two signals, whereas the second method is based on a pointwise detection of phase relations.

The continuous phase difference between two signals s_1 and s_2 can be defined in a consistent way by means of the analytic signal approach [10]. This technique provides us with the *instantaneous* phase and amplitude of an arbitrary signal $s(t)$. The analytic signal is a complex function of time, $\zeta(t)=s(t)+j\tilde{s}(t)=A(t)e^{j\phi_H(t)}$, where the function $\tilde{s}(t)$ is the Hilbert transform (HT) of $s(t)$

$$\tilde{s}(t)=\pi^{-1}\,\mathrm{P}\int_{-\infty}^{\infty}\frac{s(\tau)}{t-\tau}d\tau \tag{3}$$

(where P means that the integral is taken in the sense of the Cauchy principal value). The instantaneous phase $\phi_H(t)$ of the signal $s(t)$ is thus defined in a unique way. As the HT can be easily calculated numerically, the phase difference of two signals $s_1(t)$ and $s_2(t)$ can be obtained as

$$\phi_1(t)-\phi_2(t)=\arctan\frac{\tilde{s}_1(t)s_2(t)-s_1(t)\tilde{s}_2(t)}{s_1(t)s_2(t)+\tilde{s}_1(t)\tilde{s}_2(t)}. \tag{4}$$

This way, we calculate normalized phase differences from experimental data: $\Delta\phi=(\phi_1-\phi_2)/2\pi$. In all subjects we observed the theoretically predicted tracking movement patterns as shown in Fig. 1.

Another approach to detect qualitatively different dynamical regimes is symbolic transformation [11] of the pointwise relative phase. The latter is determined at discrete time steps given by the peaks of the target signal. We denote the timing point of the jth maximum of the target signal by $t_j^{(1)}$ and the timing point of the corresponding nearest maximum of the tracking signal by $t_j^{(2)}$ With these notations the *pointwise relative phase* φ_j is given by $\varphi_j=(t_j^{(2)}-t_j^{(1)})/T$, where T is the period of the target signal. The maximum detection is not problematic because both signals are not obscured by noise. Note that we do not filter the signals.

The relative phases are transformed into a symbolic sequence $s_1,\ldots,s_N$ according to the following rule:

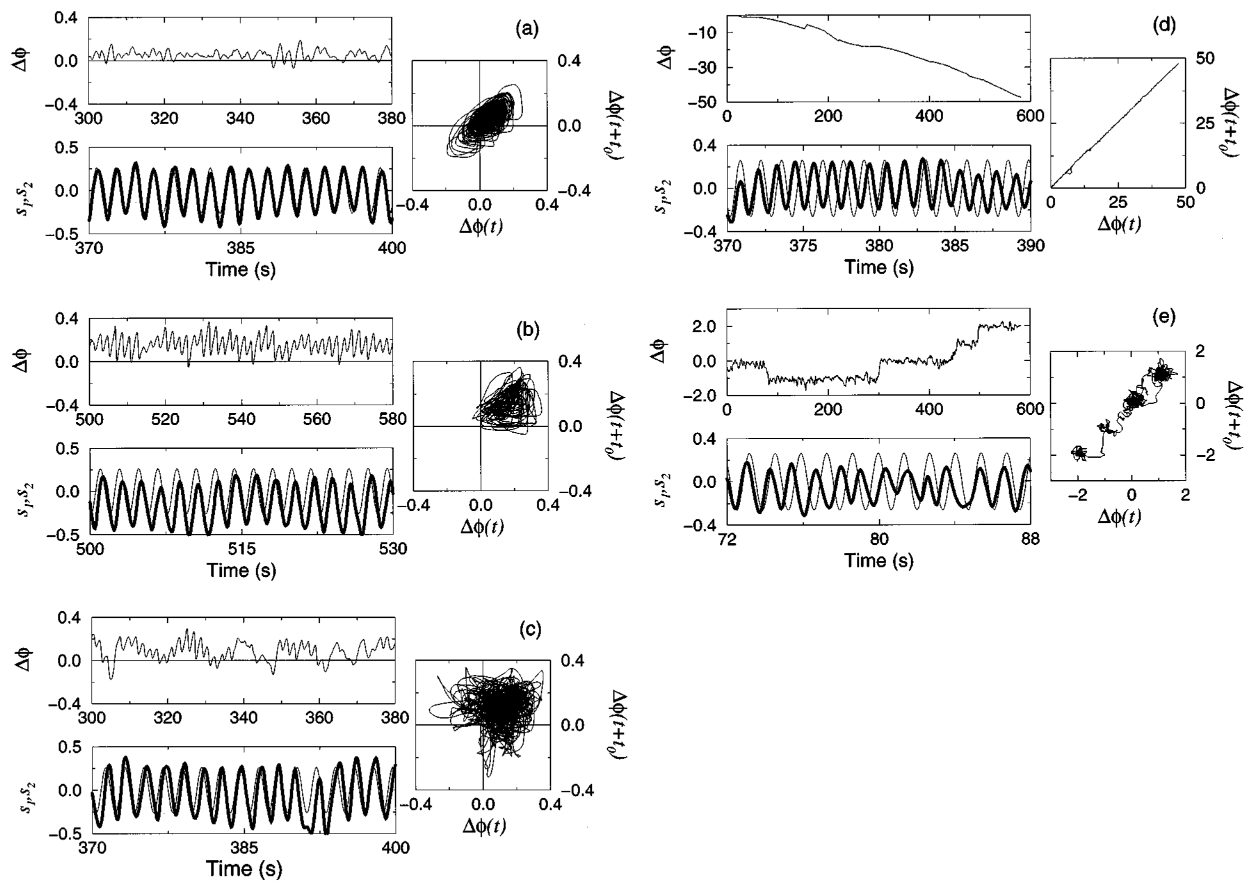

FIG. 1. Typical examples of theoretically predicted tracking movement patterns verified by HT method: Plots show $\Delta\phi$ plotted over time as well as $\Delta\phi$ phase space plot (with $t_0=\tau/4$) and original data: target signal s_1, tracking signal s_2 (boldface), both given in radians. Amplitude of s_1 corresponds to $\pm 14.5°$ manipulandum excursion. (a) Noisy shifted fixed point, where target signal advances tracking signal ($\tau_{rel}=0.15$). (b) Oscillatory tracking pattern ($\tau_{rel}=0.28$). (c) Chaoslike oscillatory tracking pattern ($\tau_{rel}=0.28$). We avoid the discussion of whether the chaoslike patterns are chaos or noisy periodic oscillations; we believe that we cannot distinguish between these two cases as the data are nonstationary. (d) Drift dynamics, where the subject passes the target nearly permanently ($\tau_{rel}=0.9$). (e) Cycle slipping. Signals plot shows how the subject passes the target once, thereby slipping from one cycle to the other ($\tau_{rel}=0.7$). Target frequency = 0.5 Hz (a), 0.5 Hz (b), 0.5 Hz (c), 0.7 Hz (d), 0.7 Hz (e).

$$s_j=\begin{cases} 0 & \text{if} \quad \varphi_j^r<-a \\ 1 & \text{if} \quad -a<\varphi_j^r<a, \\ 2 & \text{if} \quad \varphi_j^r>a \end{cases} \tag{5}$$

where a is a parameter. This one-parameter symbolic transformation reduces the amount of information but emphasizes the robust properties of the dynamics. The symbolic sequences can be visualized by assigning the symbols 0, 1, and 2 to the colors black, grey, and white respectively. Grey corresponds to a rather accurate performance of the trial, where the degree of accuracy depends on the value of a. Black and white respectively correspond to the case in which the tracking signal is in advance or behind as compared with the target signal. The symbolic pattern of all trials of one subject for a value of $a=0.025$ are shown in Fig. 2. This value has been found suitable to reflect the qualitatively different regimes. Already this simple coding rule exhibits four delay dependent dynamic regions, all of them verified by means of the HT method, too: 1. Fixed point region between $\tau_{rel}=0$ and $\tau_{rel}=0.075$, where grey dominates corresponding to rather accurate tracking performance. 2. Oscillatory tracking behavior with worse tracking performance for $\tau_{rel}=0.1$ and $\tau_{rel}=0.125$. 3. Different types of running solutions between $\tau_{rel}=0.2$ and $\tau_{rel}=0.9$. 4. Oscillatory tracking behavior for $\tau_{rel}=1$.

In order to quantify transitions between different dynamic regions, measures of complexity have to be applied to the symbolic sequences [12]. To this end we compute the Shannon entropy of the symbolic sequences for all values of the control parameter and the relative frequences of all different words of a certain length, in each sequence that can be formed with three symbols. These complexity measures enabled us to significantly quantify transitions between different dynamic regions: 1. between $\tau_{rel}=0.2$ and $\tau_{rel}=0.3$ (transition from cycle slipping to drift according to HT), 2. between $\tau_{rel}=0.5$ and $\tau_{rel}=0.6$, 3. between $\tau_{rel}=0.6$ and $\tau_{rel}=0.7$, where the HT method revealed cycle slipping evolving in five ($\tau_{rel}=0.5$), two ($\tau_{rel}=0.6$), and four ($\tau_{rel}=0.7$) cycles.

In summary, we demonstrated several delay-induced transitions in movement data. In particular, the following predictions of the model have been confirmed by the results of data analysis.

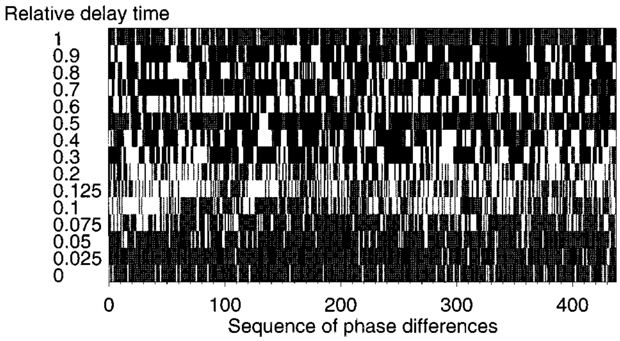

FIG. 2. Delay-induced movement patterns revealed by three symbols coding of the relative phase for $a=0.025$. The sequence of pointwise relative phase φ_j within one trial is plotted over the index j, so that (discrete) time is on the abscissa and τ_{rel} is on the ordinate. The symbol sequences of all trials are plotted starting with $\tau_{rel}=0$ at the bottom of the plot.

(i) Fixed point regime with fixed point shift occurs for small delays.

(ii) Oscillatory tracking patterns occur with increasing delay.

(iii) Running solutions take place at larger delays. In particular, delay-induced transitions between drift and different types of cycle slipping occur.

(iv) For high delays quite simple tracking dynamics (fixed point behavior or small amplitude oscillations) are observed besides the running solutions.

Minimal changes of α and β modify the model's bifurcation route dramatically. Because of the long duration of the experimental sessions, the parameters of the system cannot be considered as constant in the different trials, e.g., due to fatigue. For this reason we cannot estimate α and β by comparing our experimental data with numerical bifurcation routes for fixed α and β. Although the shift of the fixed point is clearly observed we were not able to verify Eq. (2) quantitatively for two reasons: (a) the system parameters vary during the experimental session and (b) in all subjects the number of trials with fixed point dynamics was too small. In order to investigate bifurcation scenarios as well as fixed point shift we need data in which the delay changes within a single trial (quasistatically).

Note that HT as well as symbolic dynamics aim at investigating different aspects of the phase dynamics: HT provides the continuous phase difference, whereas symbolic dynamics (in the present study) is based on the pointwise relative phase confined to the 2π interval. Nevertheless both methods succeded in detecting several theoretically predicted regimes of the phase dynamics corresponding to characteristic delay induced tracking movement patterns.

According to our results both data analysis tools presented in this article enable us to analyze tracking behavior in detail, e.g., by fitting α/β from Eq. (2) to experimental data. This way we can study tracking strategies, compensation of artificial delays, and motor learning in terms of the strength of visual versus proprioceptive feedback.

This study was supported by grants from the Deutsche Forschungsgemeinschaft (SFB 194, A5). M.R. acknowledges support from Alexander von Humboldt Foundation. G.G. acknowledges support from University of Florence.

[1] P. Tass, A. Wunderlin, and M. Schanz, J. Biol. Phys. **21**, 83 (1995).
[2] U. Langenberg *et al.*, Soc. Neurosci. Abstr. Suppl. **5**, 209 (1992).
[3] J. F. Stein and M. Glickstein, Physiol. Rev. **72**, 967 (1992).
[4] J.-L. Vercher and G. M. Gauthier, Exp. Brain Res. **90**, 599 (1992).
[5] H. Hefter *et al.*, in *Göttingen Neurobiology Report 1995*, edited by N. Elsner and R. Menzel (G. Thieme, Stuttgart, 1995), p. 233.
[6] A. Beuter, D. Laroque, and L. Glass, J. Motor Behav. **21**, 277 (1989).
[7] H. Haken, *Principles of Brain Functioning* (Springer, Berlin, 1995); J.A.S. Kelso, *Dynamic Patterns. The Self–organization of Brain and Behavior* (MIT Press, Cambridge, 1995).
[8] H. Haken, J. A. S. Kelso, and H. Bunz, Biol. Cybern. **51**, 347 (1985).
[9] L. Glass, A. Beuter, and D. Laroque, Math. Biosc. **90**, 111 (1988).
[10] P. Panter, *Modulation, Noise, and Spectral Analysis* (McGraw-Hill, New York; 1965); see also M. G. Rosenblum, A. S. Pikovsky, and J. Kurths, Phys. Rev. Lett. **76**, 1804 (1996).
[11] B.-L. Hao, Physica D **51**, 161 (1991).
[12] R. Wackerbauer *et al.*, Chaos Solitons Fractals **4**, 133 (1994); J. Kurths *et al.*, CHAOS **5**, 88 (1995).